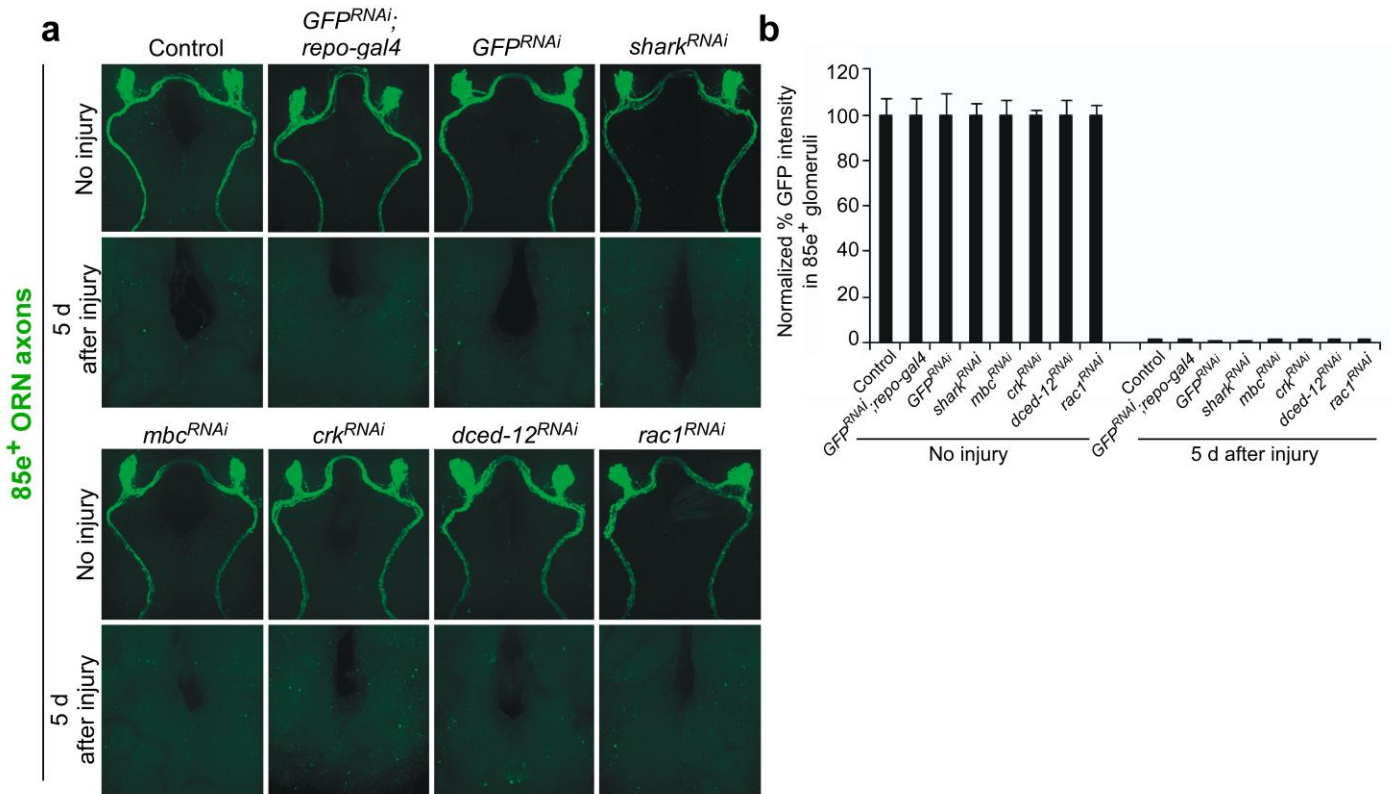


Supplementary Figure 1. Additional Crk and Rac1 RNAi constructs block glial engulfment of axonal debris

(a) The axons of OR85e-expressing ORNs were labeled with mCD8::GFP in control (*w;OR85e-mCD8::GFP/+;repo-Gal4/+*) and glial *crk*^{RNAi} (*w;OR85e-mCD8::GFP/UAS-crk^{106498RNAi};repo-Gal4/+*) or *rac1*^{RNAi} (*w;OR85e-mCD8::GFP/UAS-rac1^{49246RNAi};repo-Gal4/+*) animals. Maxillary palps were ablated or left uninjured, and the clearance of severed ORN axons from the CNS was assayed with anti-GFP antibody stains (green) 15 days after injury.

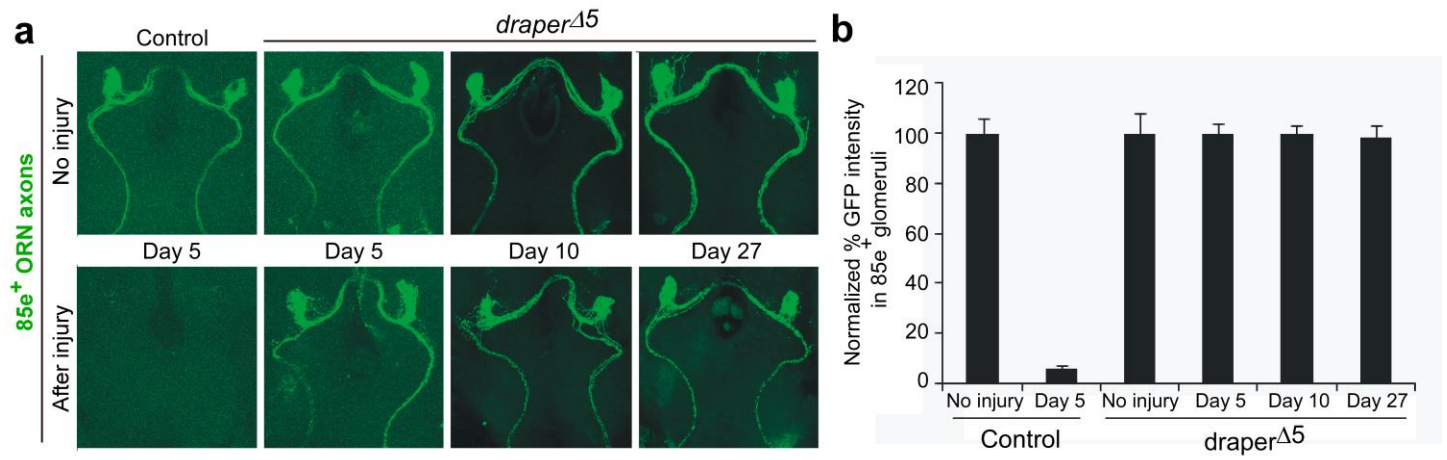
(b) Normalized quantification to uninjured cohorts from (a) Error bars represent s.e.m.; n>10 for all; ***, p<0.0001.



Supplementary Figure 2. Additional negative controls, including GFP^{RNAi}, showing normal and efficient clearance of severed axon debris

(a) The axons of OR85e-expressing ORNs were labeled with mCD8::GFP in control ($w;OR85e-mCD8::GFP/+$) and glial GFP^{RNAi} ($w;OR85e-mCD8::GFP/UAS-GFP^{RNAi};repo-Gal4/+$) animals. Glial RNAis for *shark*^{6BRNAi}, *mbc*^{16044RNAi}, *crk*^{19061RNAi}, *dced-12*^{10455RNAi}, or *rac1*^{49247RNAi} animals were crossed to the background ($w;OR85e-mCD8::GFP/+$). Maxillary palps were ablated and clearance of axonal debris from the CNS was assayed with anti-GFP antibody stains (green) 5 days after injury.

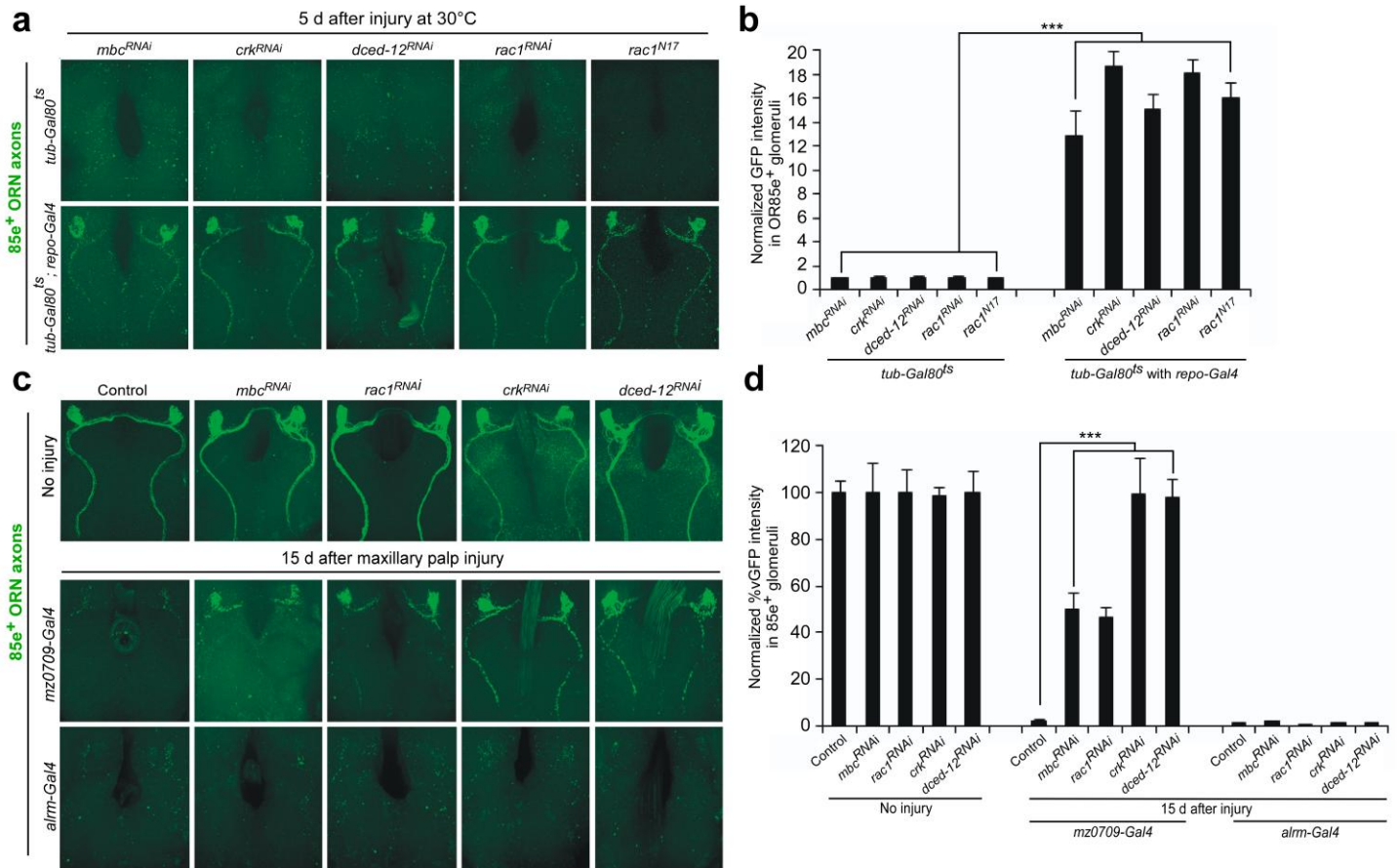
(b) Normalized quantification to uninjured cohorts from (a).; Error bars represent s.e.m.; n>10.



Supplementary Figure 3. Axonal debris persists for weeks after axotomy in *draper* mutants

(a) OR85e-expressing ORNs were labeled with mCD8::GFP in control (*w;OR85e-mcd8::GFP/+*) and *draper* null (*w;OR85e-mCD8::GFP/+; draper^{Δ5}/draper^{Δ5}*) animals. Maxillary palps were ablated and clearance of axonal debris from the CNS was assayed with anti-GFP antibody stains (green) 5, 10, and 27 days after injury. Representative confocal Z-stacks are shown.

(b) Normalized quantification to uninjured cohorts from (a) Error bars represent s.e.m.; $n > 10$ for all.



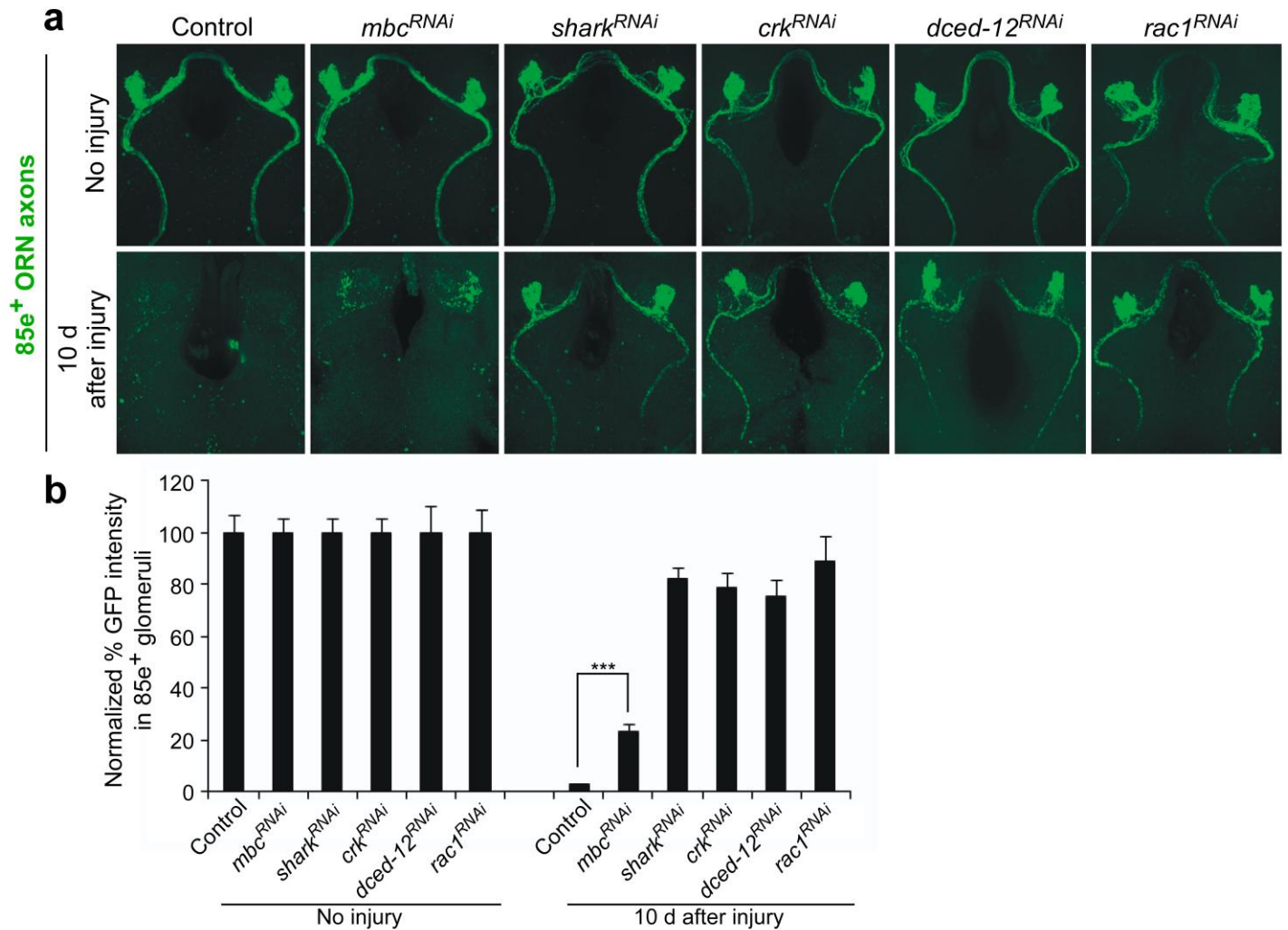
Supplementary Figure 4. Crk, dCed-12, Mbc, and Rac1 function in mature ensheathing glia to promote axon clearance

(a) Axons of OR85e-expressing ORNs were labeled with mCD8::GFP in control animals ($w;OR85e-mCD8::GFP/+;UAS-tub-Gal80^{ts}/+$ with the indicated UAS-RNAi or UAS- $rac1^{N17}$ and no driver). Crk, dCed-12, and Mbc were conditionally knocked down in adult brain glia by driving $crk^{19061RNAi}$, $dced-12^{10455RNAi}$, $mbc^{16044RNAi}$, $rac1^{49247RNAi}$, or $rac1^{N17}$ animals (in the background $w;OR85e-mCD8::GFP/UAS-tub-Gal80^{ts};repo-Gal4/+$). Animals were raised at 18°C until eclosion then maintained at 30°C for 7 days, at which point maxillary palps were ablated, and the clearance of severed axons was assayed 5 days later with anti-GFP (green).

(b) Normalized quantification to control from (a), Error bars represent s.e.m.; $n > 10$ for all; *** $p < 0.0001$.

(c) Crk, dCed-12, Mbc, and Rac1 function was knocked down in subsets of neuropil-associated glia using the ensheathing glial driver, $mz0709-Gal4$ or astrocytic glial driver, $alrm-Gal4$. Axon clearance was assayed in control animals ($w;OR85e-mCD8::GFP/+;mz0709-Gal4/+$ or $w;OR85e-mCD8::GFP/+;alrm-Gal4/+$) and glial RNAi's for $crk^{19061RNAi}$, $dced-12^{10455RNAi}$, $mbc^{16044RNAi}$, $rac1^{49247RNAi}$, and $rac1^{N17}$ animals (in the background: $w;OR85e-mCD8::GFP;mz0709-Gal4/+$ or $w;OR85e-mCD8::GFP;alrm-Gal4/+$) at the indicated time points with anti-GFP (green) 15 days after axotomy.

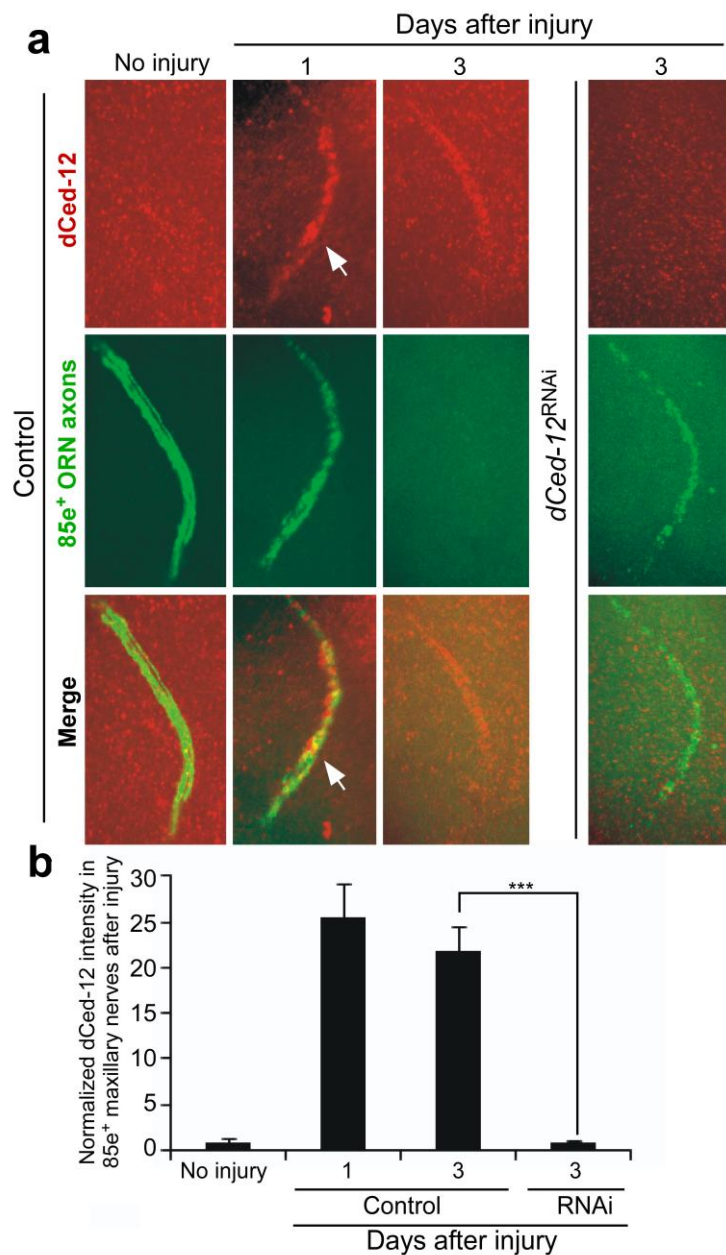
(d) Normalized quantification to uninjured cohorts from (c) Error bars represent s.e.m.; $n > 10$; *** $p < 0.0001$.



Supplementary Figure 5. Driving RNAi against known engulfment genes with the novel ensheathing glial driver, *TIFR-Gal4*, leads to persistent axon debris after injury

(a) The axons of OR85e-expressing ORNs were labeled with mCD8::GFP in control (*w;OR85e-mCD8::GFP/+;TIFR-Gal4/+*) animals. Mbc, Shark, Crk, dCed-12, and Rac1 were conditionally knocked down in adult brain glia by driving *mbc^{16044RNAi}*, *shark^{6BRNAi}*, *crk^{19061RNAi}*, *dced-12^{10455RNAi}*, or *rac1^{49247RNAi}* in the background (*w;OR85e-mCD8::GFP/+;TIFR-Gal4/+*). Maxillary palps were ablated and clearance of axonal debris from the CNS was assayed with anti-GFP antibody stains (green) 10 days after injury.

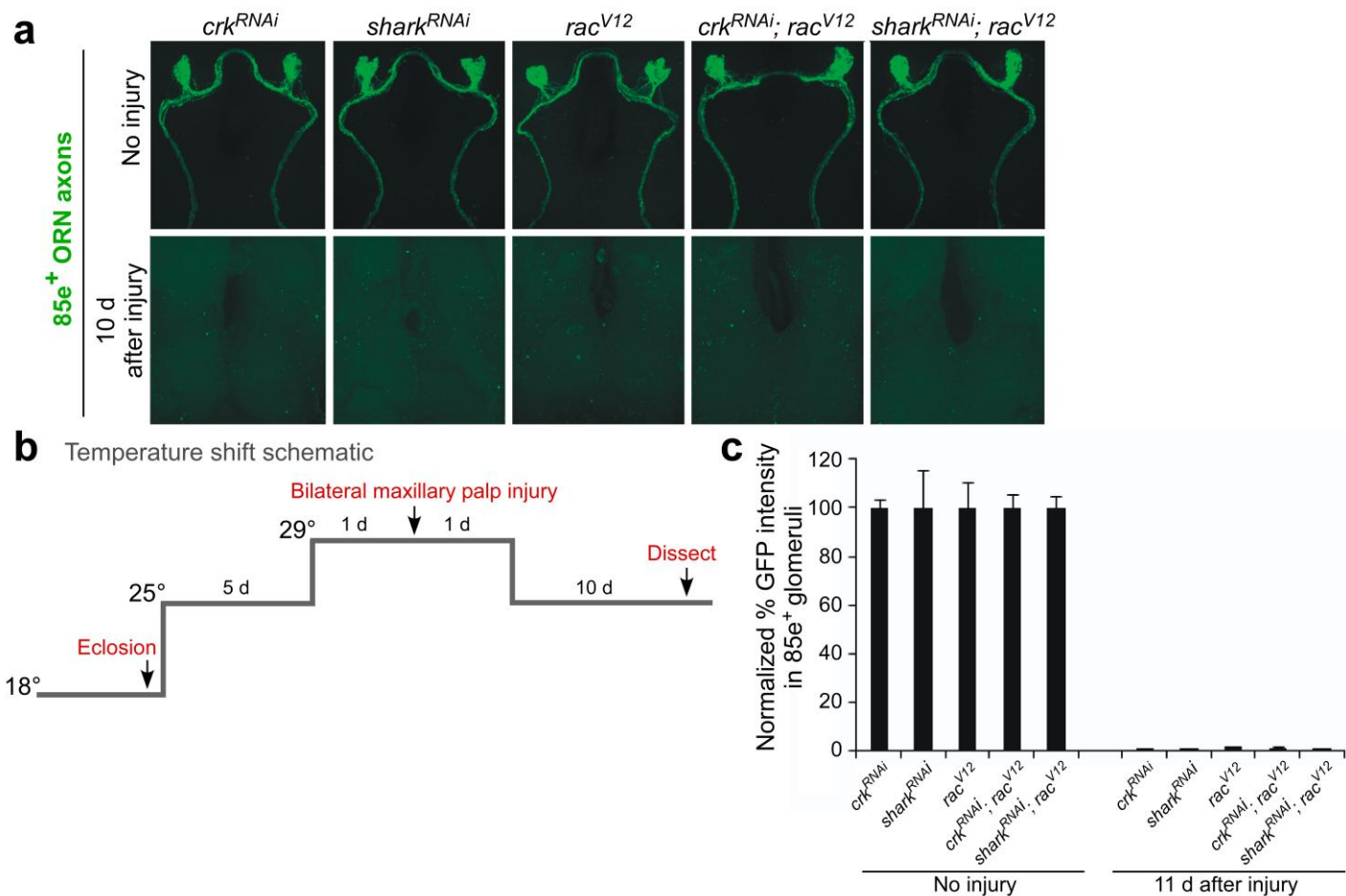
(b) Normalized quantification to uninjured cohorts from (a) Error bars represent s.e.m.; n>10; *** p<0.0001.



Supplementary Figure 6. dCed-12 localizes to severed axons during glial phagocytosis

(a) Control animals (*w;OR85e-mCD8::GFP/+;repo-Gal4/+*) and those with glia-specific knockdown of *dced-12* (*w;OR85e-mCD8::GFP/+;repo-Gal4/UAS-dced-12^{10455RNAi}*) were assayed for expression of dCed-12 (red). Axons were visualized with anti-GFP (green). Left, uninjured maxillary nerve; center, maxillary nerve 1 or 3 days after maxillary palp ablation; right, maxillary nerve in *dced-12^{RNAi}* animals 3 days after injury. White arrows denote dCed-12 antibody localizing to degenerating maxillary nerve axons (merge).

(b) Normalized quantification to uninjured cohorts from (a) Error bars represent s.e.m.; $n > 10$; *** $p < 0.0001$.

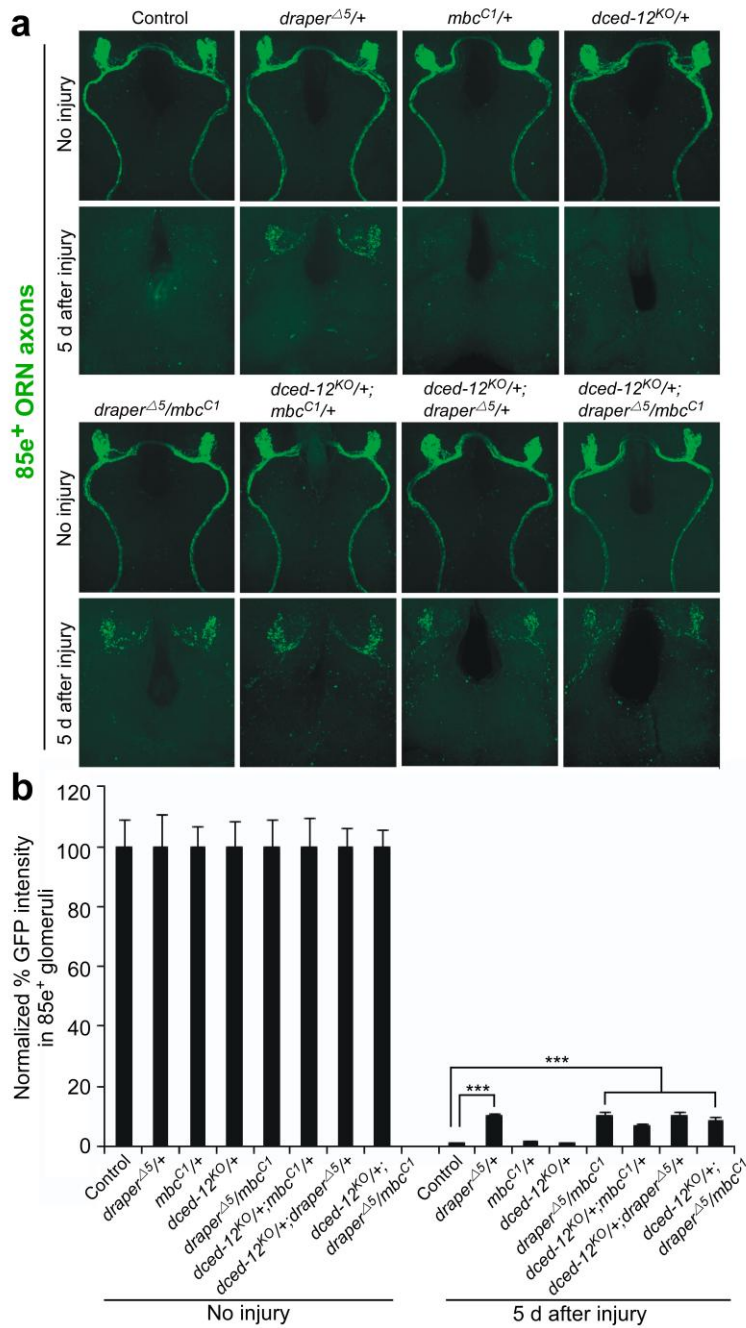


Supplementary Figure 7. Additional controls for constitutive active Rac rescue of *shark^{RNAi}* and *crk^{RNAi}* axon clearance defects

(a) OR85e-expressing ORNs were labeled with mCD8::GFP in control (*w;OR85e-mCD8::GFP/+* and glial RNAi for *crk* (*w;OR85e-mCD8::GFP, UAS-crk^{106498RNAi}*) and *shark* (*w;OR85e-mCD8::GFP, UAS-shark^{6bRNAi}*) with or without the constitutive active *rac^{V12}* (*w;OR85e-mCD8::GFP; UAS-crk^{106498RNAi}; rac^{V12}/+* and *w;OR85e-mCD8::GFP, UAS-shark^{6bRNAi}; rac^{V12}/+* and *w;OR85e-mCD8::GFP/+; rac^{V12}/+*).

Maxillary palps were bilaterally ablated and clearance of axonal debris was assayed with anti-GFP antibody stains (green) 11 days after injury, according to the temperature shift protocol outlined in (b).

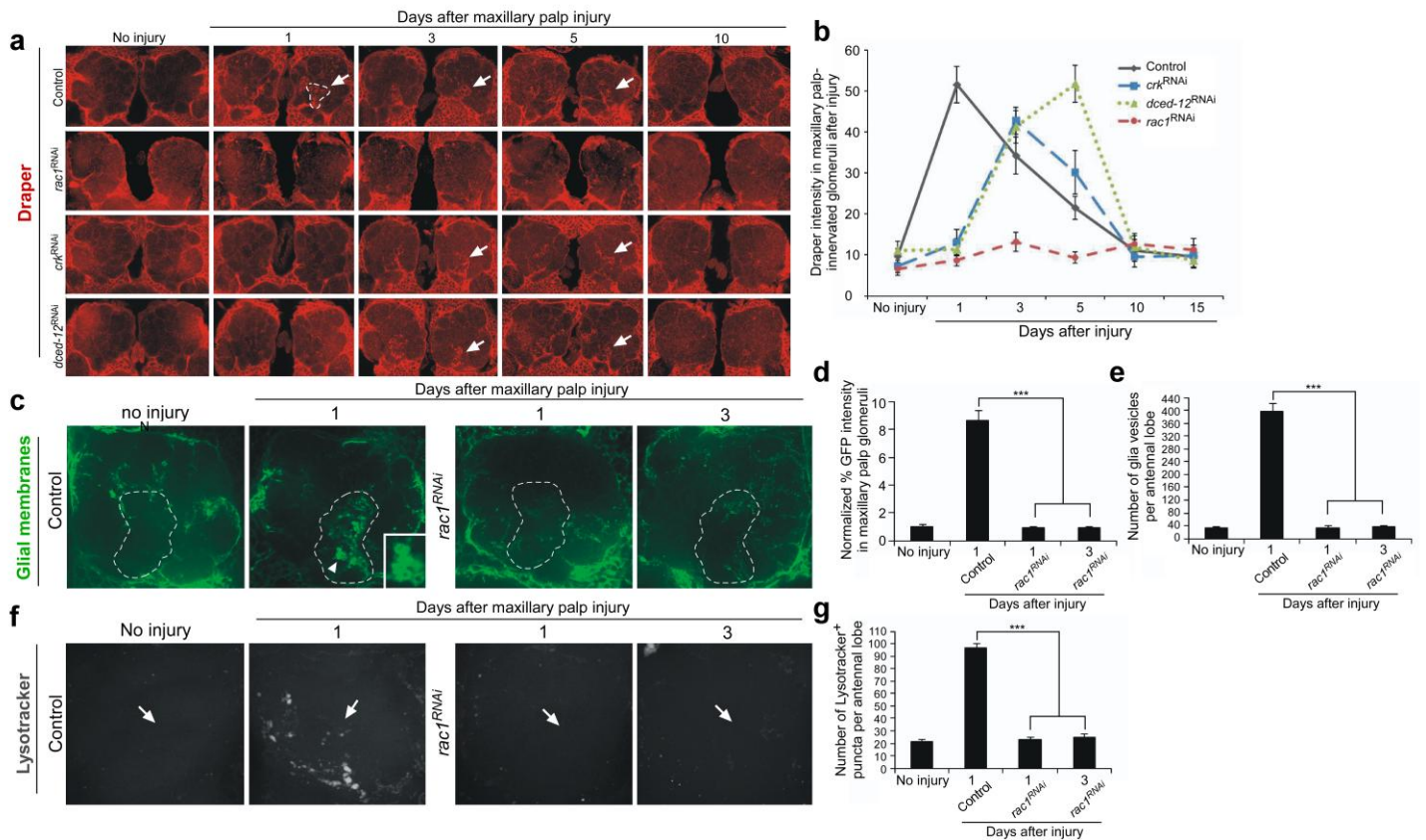
(c) Normalized quantification to uninjured cohorts from (a); Error bars represent s.e.m.; $n > 10$.



Supplementary Figure 8. *mbc*, *dced-12*, and *draper^{Δ5}* do not exhibit dominant genetic interactions in ORN axon clearance assays.

(a) OR85e-expressing ORN axons were labeled in control (*w*; *OR85e-mCD8::GFP/+*) animals and in *mbc^{C1}*, *dced-12^{KO}*, or *draper^{Δ5}* heterozygous mutant backgrounds, maxillary palps were ablated, or left uninjured, and clearance of axons (anti-GFP, green) was assayed after 5 days.

(b) Normalized quantification to uninjured controls from (a); Error bars represent s.e.m.; n>10; ***, P<0.0001.



Supplementary Figure 9. *Rac1* phenocopies Draper and is required to promote glial activation

(a) Control animals (*w;OR85e-mCD8::GFP/+;repo-Gal4/+*) and those with glia-specific knockdown of *rac1*, *dced-12*, or *crk* (*w,UAS-rac1⁴⁹²⁴⁷RNAi/OR85e-mCD8::GFP;repo-Gal4/+;w;OR85e-mCD8::GFP/+;repo-Gal4/UAS-dced-12¹⁰⁴⁵⁵RNAi*, or *w;OR85e-mCD8::GFP/UAS-crk¹⁹⁰⁶⁷RNAi/+;repo-Gal4/+*) were assayed for injury-induced recruitment of Draper (arrows) to maxillary-palp innervated glomeruli (red, dotted outline) 0, 1, 3, 5, 10, and 15 days after injury.

(b) Normalized quantification to control of Draper intensity in maxillary-palp-innervated glomeruli (dotted outline) from (a). Error bars represent s.e.m.; $n > 10$.

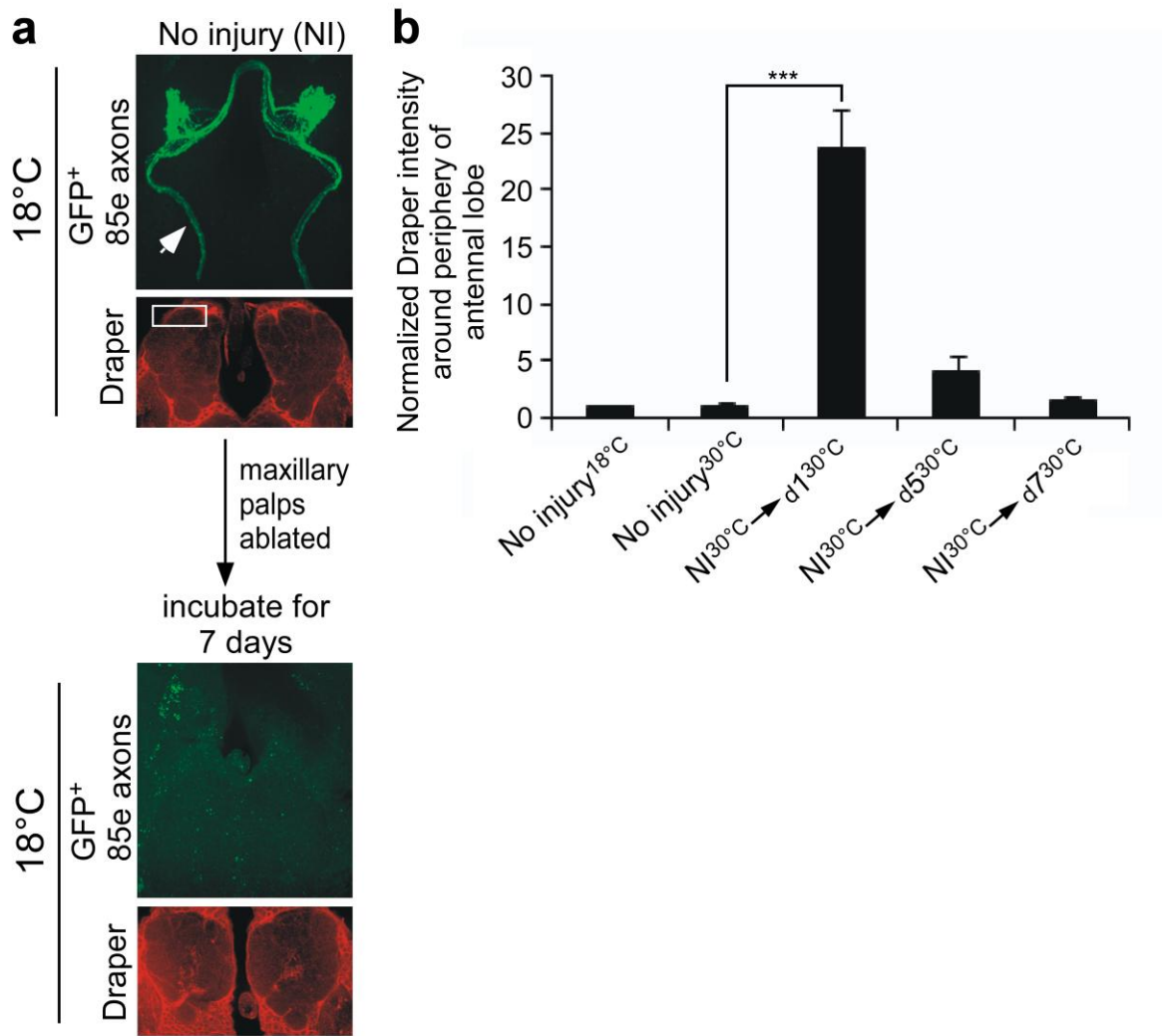
(c) Glial membranes were labeled with membrane-tethered GFP in control (*w;UAS-mcd8::GFP/+;TIFR-Gal4/+*) and those with glia-specific knockdown of *rac1* (*w;UAS-mcd8::GFP/UAS-rac1⁴⁹²⁴⁷RNAi;TIFR-Gal4/+*) were assayed for injury-induced recruitment of glial membranes and formation of glial vesicles (arrowhead) to maxillary-palp innervated glomeruli after injury. Control animals were dissected uninjured or 1 day following maxillary-palp injury. Glial *rac1*^{RNAi} animals were dissected 1 and 3 days after injury. Dotted outline; maxillary-palp-innervated glomerulus used to quantify glial invasion and formation of vesicles into injured area. Corner box; high magnification view of injury-induced glial vesicles.

(d) Normalized quantification to control from (c) of glial membrane infiltration around maxillary-palp-innervated glomeruli.

(e) Quantification from (c) of the total number of glial vesicles in maxillary-palp glomeruli.; Error bars represent s.e.m.; $n > 10$; ***, $P < 0.0001$.

(f) Lysosomal activity was labeled with Lysotracker Red (pseudo-colored grey) in uninjured control animals (*w;TIFR-Gal4/+*) or 1 day following maxillary-palp injury and in glial RNAi animals for *rac1* (*w;UAS-rac1⁴⁹²⁴⁷RNAi;TIFR-Gal4/+*) 1 or 3 days after injury. Animals were assayed for the formation of Lysotracker positive puncta throughout individual antennal lobes (pictured). Arrows; approximate location of 85e-innervated maxillary-palp glomeruli.

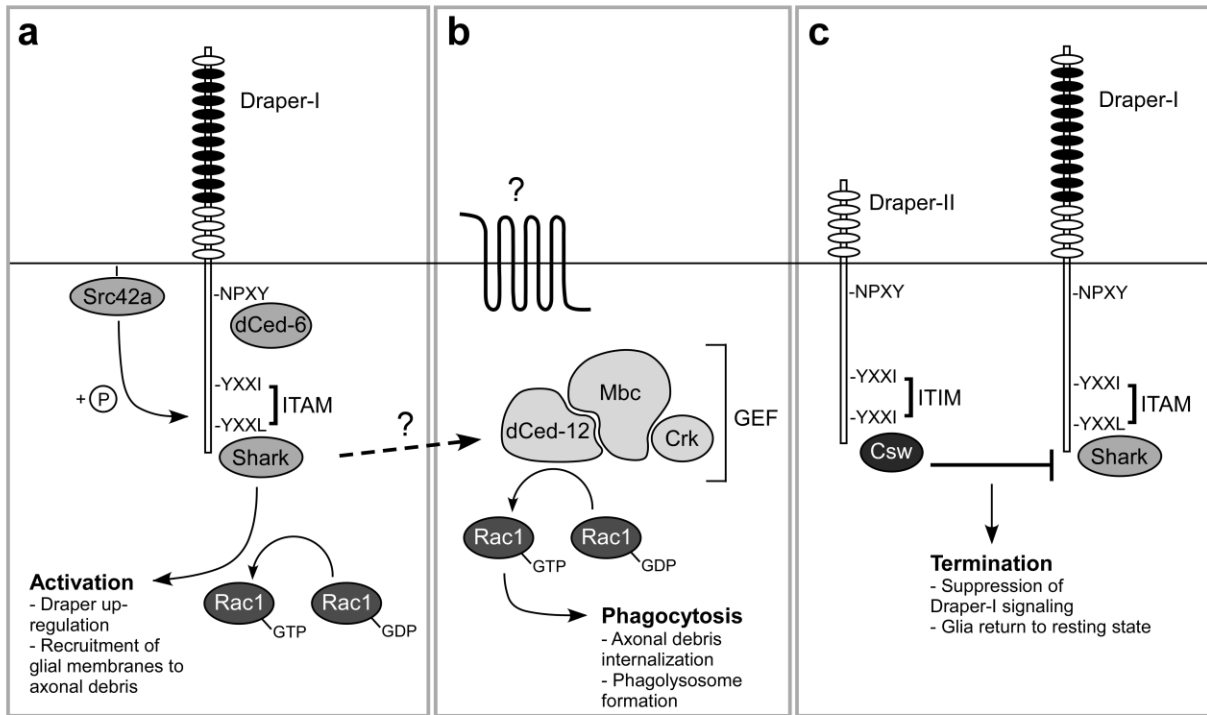
(g) Normalized quantification to control of antennal lobe lysosomal puncta data from (f).; Error bars represent s.e.m.; $n > 10$; ***, $P < 0.0001$.



Supplementary Figure 10. Severed axons as engulfment targets—Additional controls for temperature shifts and clearance windows in *shi^{ts}* animals

(a) Control animals (*w;OR85e-mCD8::GFP/UAS-shibire^{ts};mz0709-Gal4/+*) were raised at the permissive temperature, 18°C, and kept at 18°C for 7 days after eclosion. Animals were left uninjured or injured via bilateral maxillary palp ablation and assayed for Draper expression (red) and axon debris clearance (anti-GFP; green) 7 days after injury at 18°C. Z-stacks (axons) and single Z-sections (Draper⁺ glia) are shown.

(b) Normalized quantification to cohort controls of basal Draper expression around the periphery of the antennal lobe before injury (NI) or 1, 5, and 7 days after injury (D1, D5, D7) at 30°C from experimental groups described in (a) and (Figure 7a). Box from (a); representative area used to quantify peripheral antennal lobe expression of Draper. Error bars represent s.e.m.; *n*>10; ***, *p*<0.0001.



Supplementary Figure 11. Model of glial activation, phagocytosis, and termination in response to axonal injury and degeneration in the *Drosophila* CNS

a) Glial activation begins with Draper-I binding an unknown injury-induced axonal ligand. Activated Draper through an ITAM/Src42a/Shark tyrosine kinase cascade, the adaptor protein dCed-6, and ultimately Rac1. Draper expression is upregulated, and Draper, dCed-6, and glia membranes are recruited to axonal debris.

b) The Crk/Mbc/dCed-12 GEF activates Rac1 to promote phagocytosis and digestion of axonal debris. Whether Crk/Mbc/dCed-12 act downstream of Draper or another unidentified receptor remains unclear.

c) Draper-II, an alternative splice variant, inhibits glial engulfment function through the tyrosine phosphatase Corkscrew (Csw), which reduces levels of phosphorylated Shark, thereby terminating injury-induced glial responses and allowing glia to return to a resting state.